Monograph:
Peng, Z.K., Lang, Z.Q., Billings, S.A. et al. (2005) Frequency domain energy transfer properties of bilinear oscillators under harmonic loadings. Research Report. ACSE Research Report no. 909 . Automatic Control and Systems Engineering, University of Sheffield

Frequency Domain Energy Transfer Properties of Bilinear Oscillators under Harmonic Loadings

Z K Peng, Z Q Lang, S A Billings, and Y. Lu

Department of Automatic Control and Systems Engineering
The University of Sheffield
Mappin Street, Sheffield
S1 3JD, UK

Research Report No. 909
October 2005

Frequency Domain Energy Transfer Properties of Bilinear Oscillators under Harmonic Loadings

Z.K. Peng, Z.Q. Lang, S. A. Billings, and Y. Lu

Department of Automatic Control and Systems Engineering, University of Sheffield
Mappin Street, Sheffield, S1 3JD, UK
Email: z.peng@sheffield.ac.uk; z.lang@sheffield.ac.uk

Abstract: In this paper, the energy transfer phenomenon of bilinear oscillators in the frequency domain is analyzed using the new concept of Nonlinear Output Frequency Response Functions (NOFRFs). The analysis provides insight into how new frequency generation can occur using bilinear oscillators, and reveals, for the first time, that it is the resonant frequencies of the NOFRFs that dominate the occurrence of this well-known nonlinear behaviour. The results are of significance for the design and fault diagnosis of mechanical systems and structures which can be described by a bilinear oscillator model.

1 Introduction

There are abundant dynamical systems with nonlinear components in engineering. For example, vibration components with clearances and motion limiting stop or vibration components with fatigue damage, which cause abrupt changes of the damping and stiffness coefficients, represent a significant portion of these systems. In practice, bilinear oscillators can be used to model some of these nonlinear mechanical components [1]-[13]. To investigate the motion of an articulated mooring tower, Thampson *et al*. [1] modelled the system as a bilinear oscillator that has different stiffness for positive and negative deflections due to the slackening of mooring lines. A comparison between the model responses and experimental results showed a good agreement. Based on the same model, Gerber and Engelbrecht [2] studied the response of an articulated mooring tower driven by irregular seas, and Huang, Krousgrill and Rajaj [3] studied the dynamic response of an offshore structure subjected to a nonzero mean, oscillatory fluid flow where the particular interest was the interaction between the bilinear stiffness characteristic and the asymmetric hydrodynamic drag force. When investigating the behaviour of an articulated offshore platform, Choi and Lou [4] modelled the structure as a SDOF upright pendulum with bilinear springs at the top. The springs have different stiffness for positive and negative displacement (bilinear oscillator). Wilson and Gallis [5] modelled a common multi-bay, multi-story scaffold with loose tube-in-tube connecting joints as a plane structure in sway and evaluated the essential dynamic characteristics when subjected to lateral base excitations. Their investigations were based on a two-degree of freedom model with a lumped mass where the loose restraining joint between adjacent stories was treated as a bilinear stiffness. Butcher [6] investigated the effects of a clearance or interference in mechanical systems on the normal mode frequencies of a n-DOF system with bilinear stiffness without damping. The bilinear model has also been widely used to model cracks occurring in mechanical structures or rotors where the size of crack is often expressed as the stiffness ratio. Zastrau [7] demonstrated the bilinear behaviour by using the finite element method to determine the dynamic response of a simply supported beam. Friswell and Penny [8] studied the non-linear behaviour of a beam with a closing crack and then analyzed the forced response to a harmonic excitation at a frequency near the first natural frequency of the beam using a numerical integration method. The results highlighted the presence of superharmonic components in the response spectrum, a common property for non-linear systems. Sundermeyer and Weaver [9] exploited the weakly non-linear character of a cracked vibrating beam. Their studies supported the possibility that the bilinear behaviour of a fatigue crack can be exploited for the purposes of non-destructive evaluation. Based on a bilinear crack model, Chati, Rand and Mukherjee [10] used perturbation methods to obtain the non-linear normal modes of vibration and the associated period of the motion, and the results justified the definition of the bilinear frequency as the effective natural frequency. Rivola and White [11] employed the bilinear oscillator model to simulate the nonlinear behaviour of a beam with a closing crack and used the bispectrum to analyze the system response. They found that the normalized bispectrum shows high sensitivity to the bilinear nature of the crack. In cracked rotor studies [12][13], the cracked element can often be modelled as a weight-loaded hinge, and if the hinge is weight dominant, then it can further be represented as a spring element with a bilinear stiffness.

It can be seen that the bilinear oscillator is of great importance in the modeling of the nonlinear phenomena occurring in mechanical structures and machines. Accurate knowledge of this oscillator is helpful in the design, control and fault detection of these systems. A number of analytical and numerical studies on bilinear oscillators have appeared in the literature. Natsiavas [14] applied an analytical procedure to determine the exact, single-crossing, periodic response of a similar class of harmonically excited piecewise linear oscillators whose damping and restoring force are bilinear functions of the system velocity and displacement. Chu and Shen [15] employed two square wave functions to model the stiffness change in bilinear oscillators, and proposed a new closed-form solution for bilinear oscillators under low-frequency excitation. Bayly [16] derived an analytical relationship between the strength of a weak stiffness discontinuity and the magnitudes of superharmonic peaks in the output Fourier spectrum of a bilinear oscillator. Since bilinear oscillators are nonlinear, they exhibit much of the complicated phenomena associated with nonlinear systems. All the above mentioned research studies on bilinear oscillators have shown that considerable harmonic components can be generated in the spectrum of the response when a bilinear oscillator is subjected to a sinusoidal force excitation. The generation of higher harmonic components implies that some energy of the input signal is transferred from the input frequency modes to modes at other frequency locations. The conventional Frequency Response Function (FRF) can not explain why and how the energy shift occurs in bilinear oscillators as the definition of the classical frequency response is based on linear systems in which the possible output frequencies at steady state are exactly the same as the frequencies of the input.

This paper is dedicated to the study of the frequency domain energy transfer properties of bilinear oscillators using a new concept recently developed by the authors known as Nonlinear Output Frequency Response Functions (NOFRFs) [17]-[20]. The NOFRFs are a one dimensional function of frequency, which allow the analysis of nonlinear systems to be implemented in a manner similar to the analysis of linear system frequency responses. Consequently, the NOFRF based analysis in the present study not only provides new insight into how nonlinear phenomena such as new frequency generations occur with bilinear oscillators, but also reveals that it is the resonances of the NOFRFs that dominate the occurrence of the well-known nonlinear behaviour. Simulation studies justify the conclusions, and demonstrate the significance of the NOFRF based analysis. The results achieved are of significance for the design and fault diagnosis of mechanical systems and structures which can be described by a bilinear oscillator model.

2 Bilinear Oscillator Model

The bilinear oscillator is a simple and effective model that can interpret many nonlinear phenomena in mechanical structures and machines. Figure 1 shows a SDOF bilinear oscillator whose corresponding motion can be expressed as

$$\begin{cases} m\ddot{x} + c\dot{x} + \alpha kx = f(t) & x \geq 0, \\ m\ddot{x} + c\dot{x} + kx = f(t) & x < 0, \end{cases} \tag{1}$$

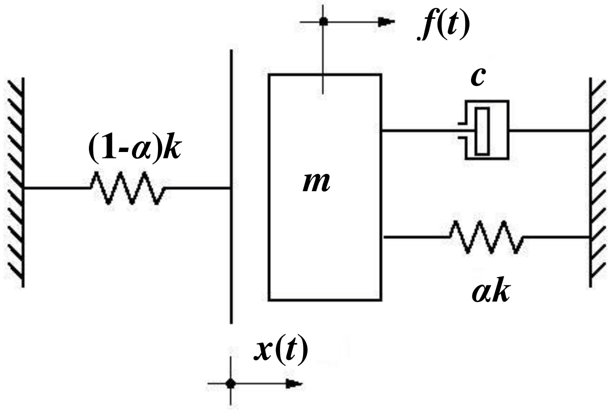

Figure 1. bilinear oscillator model

where m and c are the object mass and damping coefficient respectively; x(t) is the displacement; k is the stiffness; α is known as the stiffness ratio ($0 \le \alpha \le 1$). $f(t)$ is the external force exciting the model. Obviously, if the stiffness ratio α is equal to one, then the model is linear. When excited by a sinusoidal force, the response will be a sinusoidal function of the same frequency. Otherwise, if α is smaller than one, the response is expected to contain several harmonics of the excitation frequency. Define $S(x)$ as the restoring force of a bilinear oscillator as follows

$$S(x) = \begin{cases} \alpha kx & x \geq 0, \\ kx & x < 0, \end{cases} \tag{2}$$

Obviously $S(x)$ is a piecewise linear continuous function of displacement x illustrated in Figure 2.

In mathematics, the Weierstrass Approximation Theorem [21] guarantees that any continuous function on a closed and bounded interval can be uniformly approximated on that interval by a polynomial to any degree of accuracy. This theorem is expressed as

If $f(x)$ is a continuous real-valued function on $[\bar{a}, \bar{b}]$ and if any $\varepsilon > 0$ is given, then there exists a polynomial $P(x)$ on $[\bar{a}, \bar{b}]$ such that $|f(x) - P(x)| < \varepsilon$ for all $x \in [\bar{a}, \bar{b}]$.

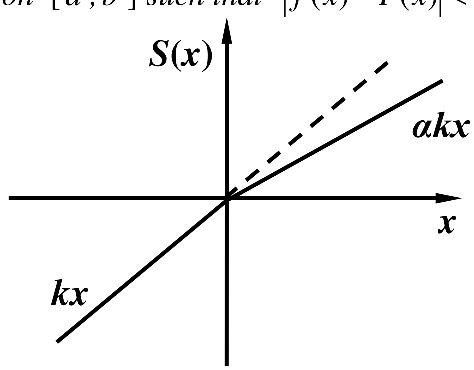

Figure 2. The restoring force of a bilinear oscillator

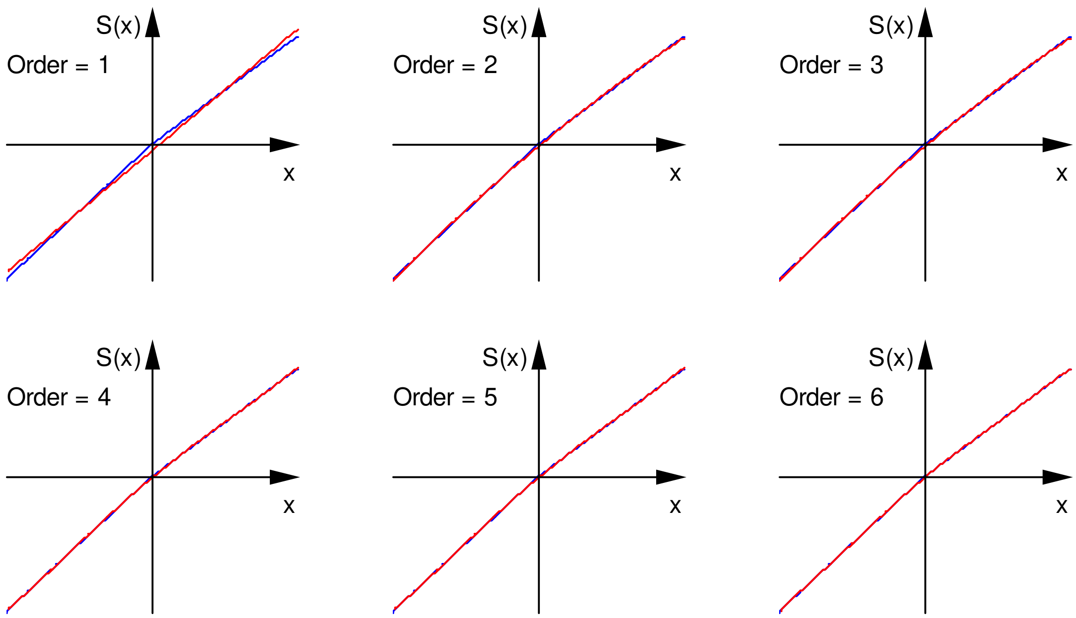

Figure 3. Approximation of $S(x)$ ($\alpha = 0.8$) with polynomials

Since the restoring force $S(x)$ is a continuous function of displacement x, it can be well approximated by a polynomial. Figure 3 gives the results of using polynomials with different orders to approximate $S(x)$ where the stiffness ratio α is taken as 0.8. It can be seen that a fourth order polynomial can fit $S(x)$ very well. If using a polynomial $P(x)$ to replace for $S(x)$ and ignoring the tiny approximation error, the SDOF model Equation (1) can be rewritten as

$$m\ddot{x} + c\dot{x} + P(x) = f(t) \tag{3}$$

where

$$P(x) = \sum_{i=1}^{\overline{N}} c_i k x^i \tag{4}$$

where $\overline{N}$ is the order of the approximating polynomial, and kc_i , $i = 1, \cdots, \overline{N}$ are the polynomial coefficients.

Table 1 The polynomial approximation result for a bilinear oscillator

α \ c	c_1	c_2	c_3	c_4
1.00	1.0000	0.0000	0.0000	0.0000
0.95	0.9750	-0.0409	0.0000	0.0204
0.90	0.9500	-0.0818	0.0000	0.0407
0.85	0.9250	-0.1228	0.0000	0.0611
0.80	0.9000	-0.1637	0.0000	0.0814

The model described by Equation (3) is an extensively studied polynomial-type nonlinear system where the term $c_1 kx$ represents the linear part and the other high order terms represent the nonlinear part. For the bilinear oscillator model, the polynomial coefficients are determined by the stiffness ratio *α*. Table 1 shows the results of using a fourth order polynomial to approximate the bilinear oscillator with different stiffness ratios. It is known from Table 1 that all coefficients, apart from c_1, will increase with a decrease of *α*. This means that the nonlinear strength of the bilinear oscillator will increase with the decrease of *α*. It is worth to noting that except for c_1, the values of $c_2 \ldots$ and $c_{\overline{N}}$ also depend on the range of *x* which the polynomial approximation is defined. In the case shown in Table 1, this range of *x* is [-1, 1].

For the free undamped vibration of bilinear oscillators, its effective natural frequency can be substituted with a bilinear frequency ω_B [11], as

$$\omega_B = 2\omega_0\omega_1 / (\omega_0 + \omega_1) \tag{5}$$

where

$$\omega_0 = \sqrt{k/m} \text{ and } \omega_1 = \sqrt{\alpha k/m} \tag{6}$$

Therefore

$$\omega_B = \frac{2\sqrt{\alpha}}{(1+\sqrt{\alpha})}\sqrt{\frac{k}{m}} = \frac{2\sqrt{\alpha}}{(1+\sqrt{\alpha})}\omega_0 \tag{7}$$

For the polynomial-type nonlinear system (3), the natural frequency of the linear part can be defined as

$$\omega_L = \sqrt{c_1 k/m} = \sqrt{c_1}\,\omega_0 \tag{8}$$

Table 2 shows a comparison between ω_L and ω_B under different stiffness ratios. It can be seen that the ω_L is a good approximation of ω_B. To a certain extent, this further justifies using a polynomial-type nonlinear model to describe a bilinear oscillator.

Table 2. Comparison between ω_L and ω_B

α	$\omega_L(\times\omega_0)$	$\omega_B(\times\omega_0)$	$\lvert\omega_B - \omega_L\rvert / \omega_B$
1.00	1.0000	1.0000	0.0000%
0.95	0.9874	0.9872	0.0203%
0.90	0.9747	0.9737	0.1027%
0.85	0.9618	0.9594	0.2501%
0.80	0.9487	0.9443	0.4660%

For polynomial-type nonlinear systems, a powerful analysis tool called the Nonlinear Output Frequency Response Function (NOFRF) has been used to study system behaviours [19]. The objective of the present study is to use the NOFRF concept to study the frequency domain energy transfer properties of bilinear oscillators under harmonic loading.

3 Nonlinear Output Frequency Response Functions (NOFRFs)

3.1 NOFRFs under General Inputs

NOFRFs were recently proposed and used to investigate the behaviour of structures with polynomial-type non-linearities [19]. The definition of NOFRFs is based on the Volterra series. The Volterra series extends the familiar concept of the convolution integral for linear systems to a series of multi-dimensional convolution integrals.

For a linear system, with input $u(t)$ and output $y(t)$, the input and output relationship in the time domain can be described by a convolution integral, as

$$y(t) = \int_{-\infty}^{\infty} h(\tau)u(t-\tau)d\tau \tag{9}$$

In the frequency domain, the linear system input output relationship is given by

$$Y(j\omega) = H(j\omega)U(j\omega) \tag{10}$$

when the system is subject to an input where the Fourier Transform exists. In equation (10), $Y(j\omega)$ and $U(j\omega)$ are the system input and output spectrum which are the Fourier Transforms of the system time domain input $u(t)$ and output $y(t)$ respectively. It can be seen that the possible frequency components of $Y(j\omega)$ are the same as the frequencies of $U(j\omega)$.

Consider the class of nonlinear systems which are stable at zero equilibrium and which can be described in the neighbourhood of the equilibrium by the Volterra series

$$y(t) = \sum_{n=1}^{N} \int_{-\infty}^{\infty} \cdots \int_{-\infty}^{\infty} h_n(\tau_1,\ldots,\tau_n) \prod_{i=1}^{n} u(t-\tau_i)d\tau_i \tag{11}$$

where $h_n(\tau_1,\ldots,\tau_n)$ is the nth order Volterra kernel, and N denotes the maximum order of the system nonlinearity. Lang and Billings [17] have derived an expression for the output frequency response of this class of nonlinear systems to a general input. The result is

$$\begin{cases} Y(j\omega) = \sum_{n=1}^{N} Y_n(j\omega) \quad \text{for } \forall\omega \\ Y_n(j\omega) = \dfrac{1/\sqrt{n}}{(2\pi)^{n-1}} \displaystyle\int_{\omega_1+,\ldots,+\omega_n=\omega} H_n(j\omega_1,\ldots,j\omega_n) \prod_{i=1}^{n} U(j\omega_i)d\sigma_{n\omega} \end{cases} \tag{12}$$

This expression reveals how nonlinear mechanisms operate on the input spectra to produce the system output frequency response. In (12), $Y_n(j\omega)$ represents the nth order output frequency response of the system,

$$H_n(j\omega_1,...,j\omega_n)=\int_{-\infty}^{\infty}...\int_{-\infty}^{\infty}h_n(\tau_1,...,\tau_n)e^{-(\omega_1\tau_1+,...,+\omega_n\tau_n)j}d\tau_1...d\tau_n \qquad (13)$$

is the definition of the Generalised Frequency Response Function (GFRF), and

$$\int_{\omega_1+,...,+\omega_n=\omega} H_n(j\omega_1,...,j\omega_n)\prod_{i=1}^{n}U(j\omega_i)d\sigma_{n\omega}$$

denotes the integration of $H_n(j\omega_1,...,j\omega_n)\prod_{i=1}^{n}U(j\omega_i)$ over the n-dimensional hyper-plane, with the constraint of $\omega_1+\cdots+\omega_n=\omega$. Equation (12) is a natural extension of the well-known linear relationship (10) to the nonlinear case.

For linear systems, equation (10) shows that the possible output frequencies are the same as the frequencies in the input. For nonlinear systems described by equation (11), however, the relationship between the input and output frequencies is generally given by

$$f_Y=\bigcup_{n=1}^{N}f_{Y_n} \qquad (14)$$

where f_Y denotes the non-negative frequency range of the system output, and f_{Y_n} represents the non-negative frequency range produced by the nth-order system nonlinearity. This is much more complicated than that in the linear system case. For the cases where system (12) is subjected to an input with a spectrum given by

$$U(j\omega)=\begin{cases}U(j\omega) & \text{when} \quad |\omega|\in(a,b)\\ 0 & \text{otherwise}\end{cases} \qquad (15)$$

where $b>a\geq 0$. Lang and Billings [17] derived an explicit expression for the output frequency range f_Y of the systems. The result obtained is

$$\begin{cases} f_Y=f_{Y_N}\bigcup f_{Y_{N-(2p^*-1)}} \\ f_{Y_n}=\begin{cases}\bigcup_{k=0}^{i^*-1}I_k & \text{whe n } \dfrac{nb}{(a+b)}-\left\lfloor\dfrac{na}{(a+b)}\right\rfloor<1\\ \bigcup_{k=0}^{i^*}I_k & \text{whe n } \dfrac{nb}{(a+b)}-\left\lfloor\dfrac{na}{(a+b)}\right\rfloor\geq 1\end{cases} \\ i^*=\left\lfloor\dfrac{na}{(a+b)}\right\rfloor+1 \\ \text{where } \lfloor . \rfloor \text{ means to take the integer part} \\ I_k=\left(na-k(a+b),nb-k(a+b)\right) \text{ for } k=0,...,i^*-1, \\ I_{i^*}=\left(0,nb-i^*(a+b)\right)\end{cases} \qquad (16)$$

In (16) p^* could be taken as $1,2,\cdots,\lfloor N/2 \rfloor$, the specific value of which depends on the system nonlinearities. If the system GFRFs $H_{N-(2i-1)}(.)=0$, for $i=1,\cdots,q-1$, and $H_{N-(2q-1)}(.)\neq 0$, then $p^*=q$. This is the first analytical description for the output frequencies of nonlinear systems, which extends the well-known relationship between the input and output frequencies of linear systems to nonlinear cases.

Based on the above results for output frequency responses of nonlinear systems, a new concept known as Nonlinear Output Frequency Response Functions (NOFRF) was recently introduced by Lang and Billings [19]. The concept was defined as

$$G_n(j\omega)=\frac{\int_{\omega_1+,\ldots,+\omega_n=\omega} H_n(j\omega_1,\ldots,j\omega_n)\prod_{i=1}^{n}U(j\omega_i)d\sigma_{n\omega}}{\int_{\omega_1+,\ldots,+\omega_n=\omega} \prod_{i=1}^{n}U(j\omega_i)d\sigma_{n\omega}} \tag{17}$$

under the condition that

$$U_n(j\omega)=\int_{\omega_1+,\ldots,+\omega_n=\omega} \prod_{i=1}^{n}U(j\omega_i)d\sigma_{n\omega}\neq 0 \tag{18}$$

Notice that $G_n(j\omega)$ is valid over the frequency range f_{Y_n} as defined in (16).

By introducing the NOFRFs $G_n(j\omega)$, $n=1,\cdots N$, Equation (12) can be written as

$$Y(j\omega)=\sum_{n=1}^{N}Y_n(j\omega) \ =\sum_{n=1}^{N}G_n(j\omega)U_n(j\omega) \tag{19}$$

which is similar to the description of the output frequency response of linear systems. For a linear system, the relationship between $Y(j\omega)$ and $U(j\omega)$ can be illustrated as in Figure 4. Similarly, the nonlinear system input and output relationship of Equation (19) can be illustrated as in Figure 5.

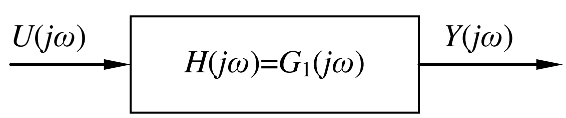

Figure 4. The output frequency response of a linear system

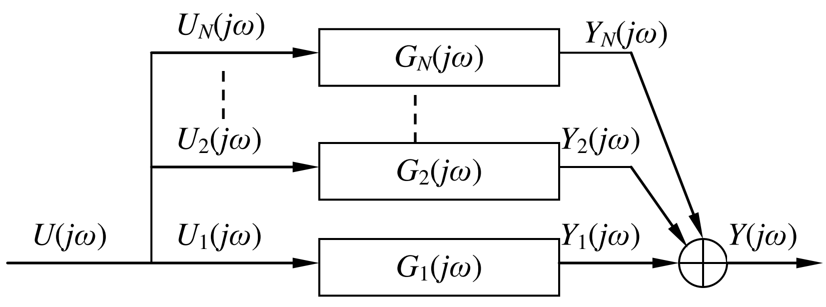

Figure 5. The output frequency response of a nonlinear system

The NOFRFs reflect a combined contribution of the system and the input to the frequency domain output behaviour. It can be seen from Equation (17) that $G_n(j\omega)$ depends not only on H_n (i=1,…,N) but also on the input $U(j\omega)$. For any structure, the dynamical properties are determined by the GFRFs H_n (i= 1,…,N). However, from Equation (13) it can be seen that the GFRF is multidimensional [22][23], which makes it difficult to measure, display and interpret the GFRFs in practice. Feijoo, Worden and Stanway [24]-[26] demonstrated that the Volterra series can be described by a series of associated linear equations (ALEs) whose corresponding associated frequency response functions (AFRFs) are easier to analyze and interpret than the GFRFs. Here, according to Equation (17), the NOFRF $G_n(j\omega)$ is a weighted sum of $H_n(j\omega_1,\ldots,j\omega_n)$ over $\omega_1+\cdots+\omega_n=\omega$ with the weights depending on the test input. Therefore $G_n(j\omega)$ can be used as alternative representation of the structural dynamical properties described by H_n. The most important property of the NOFRF $G_n(j\omega)$ is that it is one dimensional, and thus allows the analysis of nonlinear systems to be implemented in a very convenient manner very similar to the analysis of linear systems. Moreover, there is an effective algorithm [19] available which allows the estimation of the NOFRFs to be implemented directly using system input output data. The algorithm generally requires experimental or simulation results for the system under investigation under N different input signal excitations, which have the same waveforms but different intensities.

3.2 NOFRFs under Harmonic Input

Harmonic inputs are pure sinusoidal signals which have been widely used for dynamic testing of many engineering structures. Therefore, the extension of the NOFRF concept to the harmonic input case is of considerable engineering significance.

When system (11) is subject to a harmonic input

$$u(t) = A\cos(\omega_F t + \beta) \tag{20}$$

Lang and Billings [17] showed that equation (12) can be expressed as

$$Y(j\omega) = \sum_{n=1}^{N} Y_n(j\omega) = \sum_{n=1}^{N}\left(\frac{1}{2^n}\sum_{\omega_{k_1}+\cdots+\omega_{kn}=\omega} H_n(j\omega_{k_1},\cdots,j\omega_{k_n})A(j\omega_{k_1})\cdots A(j\omega_{k_n})\right) \tag{21}$$

where

$$A(j\omega) = \begin{cases} |A|\,e^{jsign(k)\beta} & if \quad \omega \in \{k\omega_F, k=\pm 1\} \\ 0 & otherwise \end{cases} \tag{22}$$

Define the frequency components of nth order output of the system as Ω_n, according to Equation (21), the frequency components in the system output can be expressed as

$$\Omega = \bigcup_{n=1}^{N} \Omega_n \tag{23}$$

and Ω_n is determined by the set of frequencies

$$\{\omega = \omega_{k_1} + \cdots + \omega_{k_n} \mid \omega_{k_i} = \pm\omega_F, i = 1, \cdots, n\} \tag{24}$$

From Equation (24), it is known that if all $\omega_{k_1}, \cdots, \omega_{k_n}$ are taken as $-\omega_F$, then $\omega = -n\omega_F$. If k of them are taken as ω_F, then $\omega = (-n+2k)\omega_F$. The maximal k is n. Therefore the possible frequency components of $Y_n(j\omega)$ are

$$\Omega_n = \{(-n+2k)\omega_F, k = 0, 1, \cdots, n\} \tag{25}$$

Moreover, it is easy to deduce that

$$\Omega = \bigcup_{n=1}^{N} \Omega_n = \{k\omega_F, k = -N, \cdots, -1, 0, 1, \cdots, N\} \tag{26}$$

Equation (26) explains why some superharmonic components will be generated when a nonlinear system is subjected to a harmonic excitation. In the following, only those components with positive frequencies will be considered.

The NOFRFs defined in Equation (17) can be extended to the case of harmonic inputs as

$$G_n^H(j\omega) = \frac{\frac{1}{2^n} \sum_{\omega_{k_1}+\cdots+\omega_{kn}=\omega} H_n(j\omega_{k_1}, \cdots, j\omega_{k_n}) A(j\omega_{k_1}) \cdots A(j\omega_{k_n})}{\frac{1}{2^n} \sum_{\omega_{k_1}+\cdots+\omega_{kn}=\omega} A(j\omega_{k_1}) \cdots A(j\omega_{k_n})} \quad n = 1, \ldots, N \tag{27}$$

under the condition that

$$A_n(j\omega) = \frac{1}{2^n} \sum_{\omega_{k_1}+\cdots+\omega_{kn}=\omega} A(j\omega_{k_1}) \cdots A(j\omega_{k_n}) \neq 0 \tag{28}$$

Obviously, $G_n^H(j\omega)$ is only valid over Ω_n defined by Equation (25). Consequently, the output spectrum $Y(j\omega)$ of nonlinear systems under a harmonic input can be expressed as

$$Y(j\omega) = \sum_{n=1}^{N} Y_n(j\omega) = \sum_{n=1}^{N} G_n^H(j\omega) A_n(j\omega) \tag{29}$$

When k of the n frequencies of $\omega_{k_1}, \cdots, \omega_{k_n}$ are taken as ω_F and the others are as $-\omega_F$, substituting Equation (22) into Equation (28) yields,

$$A_n(j(-n+2k)\omega_F) = \frac{1}{2^n} |A|^n e^{j(-n+2k)\beta} \tag{30}$$

Thus $G_n^H(j\omega)$ becomes

$$G_n^H(j(-n+2k)\omega_F)=\frac{\frac{1}{2^n}H_n(\overbrace{j\omega_F,\cdots,j\omega_F}^{k},\overbrace{-j\omega_F,\cdots,-j\omega_F}^{n-k})\,|A|^n\,e^{j(-n+2k)\beta}}{\frac{1}{2^n}|A|^n\,e^{j(-n+2k)\beta}}$$

$$=H_n(\overbrace{j\omega_F,\cdots,j\omega_F}^{k},\overbrace{-j\omega_F,\cdots,-j\omega_F}^{n-k}) \qquad (31)$$

Where $H_n(j\omega_1,...,j\omega_n)$ is a symmetric function. Therefore, in this case, $G_n^H(j\omega)$ over the nth order output frequency range $\Omega_n=\{(-n+2k)\omega_F, k=0,1,\cdots,n\}$ is equal to the GFRF $H_n(j\omega_1,...,j\omega_n)$ evaluated at $\omega_1=\cdots=\omega_k=\omega_F$, $\omega_{k+1}=\cdots=\omega_n=-\omega_F$, $k=0,\cdots,n$.

3.3 NOFRFs of Bilinear Oscillators under Harmonic Inputs

Consider the fourth-order nonlinear polynomial system used to approximate a bilinear oscillator

$$m\ddot{x}+c\dot{x}+c_1kx+c_2kx^2+c_3kx^3+c_4kx^4=f(t) \qquad (32)$$

where $c_3=0$ according to the approximation results in Table 1. By setting

$$\varsigma=\frac{c}{2\sqrt{mc_1k}},\quad \omega_L=\sqrt{\frac{c_1k}{m}},\quad \varepsilon_2=\frac{c_2}{c_1},\quad \varepsilon_3=\frac{c_3}{c_1}=0,\quad \varepsilon_4=\frac{c_4}{c_1},\quad f_0(t)=\frac{f(t)}{m}$$

Equation (32) can be expressed in a standard form

$$\ddot{x}+2\varsigma\omega_L\dot{x}+\omega_L^2x+\varepsilon_2\omega_L^2x^2+\varepsilon_4\omega_L^2x^4=f_0(t) \qquad (33)$$

The first order frequency response function can easily be determined from the linear part of Equation (33) as

$$G_1^H(j\omega)=H_1(j\omega)=\frac{1}{(j\omega)^2+2\varsigma\omega_L(j\omega)+\omega_L^2} \qquad (34)$$

The GFRF up to 4$^{\text{th}}$ order can be calculated recursively using the algorithm by Billings and Peyton Jones [31] to produce the results below.

$$H_2(j\omega_1,j\omega_2)=-\varepsilon_2\omega_L^2H_1(j\omega_1)H_1(j\omega_2)H_1(j\omega_1+j\omega_2) \qquad (35)$$

$$\begin{aligned}H_3(j\omega_1,j\omega_2,j\omega_3)=-\frac{2}{3}\omega_L^2\varepsilon_2\big[&H_1(j\omega_1)H_2(j\omega_2,j\omega_3)+H_1(j\omega_2)H_2(j\omega_1,j\omega_3)\\&+H_1(j\omega_3)H_2(j\omega_1,j\omega_2)\big]\times H_1(j\omega_1+j\omega_2+j\omega_3)\end{aligned} \qquad (36)$$

$$\begin{aligned}H_4(j\omega_1,j\omega_2,j\omega_3,j\omega_4)=-\omega_L^2H_1(j\omega_1+j\omega_2+j\omega_3+j\omega_4)\times\big[&\varepsilon_2H_{42}(j\omega_1,j\omega_2,j\omega_3,j\omega_4)\\&+\varepsilon_4H_{44}(j\omega_1,j\omega_2,j\omega_3,j\omega_4)\big]\end{aligned} \qquad (37)$$

where

$$H_{42}(j\omega_1,j\omega_2,j\omega_3,j\omega_4)=\frac{1}{2}\big[H_1(j\omega_1)H_3(j\omega_2,j\omega_3,j\omega_4)$$

$$+H_1(j\omega_2)H_3(j\omega_1,j\omega_3,j\omega_4)+H_1(j\omega_3)H_3(j\omega_1,j\omega_2,j\omega_4)$$
$$+H_1(j\omega_4)H_3(j\omega_1,j\omega_2,j\omega_3)\big]+\frac{1}{3}\big[H_2(j\omega_1,j\omega_2)H_2(j\omega_3,j\omega_4)$$
$$+H_2(j\omega_1,j\omega_3)H_2(j\omega_2,j\omega_4)+H_2(j\omega_1,j\omega_4)H_2(j\omega_2,j\omega_3)\big] \quad (38)$$

$$H_{44}(j\omega_1,j\omega_2,j\omega_3,j\omega_4)=H_1(j\omega_1)H_1(j\omega_2)H_1(j\omega_3)H_1(j\omega_4) \quad (39)$$

From Equations (35)~(39), it can be seen that $H_4(j\omega_1,j\omega_2,j\omega_3,j\omega_4)$, $H_3(j\omega_1,j\omega_2,j\omega_3)$ and $H_2(j\omega_1,j\omega_2)$ are symmetric functions. Therefore, when the system in (32) is subjected to a harmonic loading, the NOFRFs of the system can be described as

$$G_2^H(j2\omega)=H_2(j\omega,j\omega)=-\varepsilon_2\omega_L^2H_1^2(j\omega)H_1(j2\omega) \quad (40)$$

$$G_3^H(j\omega)=H_3(-j\omega,j\omega,j\omega)=\frac{2}{3}\omega_L^2\varepsilon_2^2\big[\omega_L^2H_1(j2\omega)+2\big]H_1^2(j\omega)\,|\,H_1(j\omega)\,|^2 \quad (41)$$

$$G_3^H(j3\omega)=H_3(j\omega,j\omega,j\omega)=2\omega_L^4\varepsilon_2^2H_1^3(j\omega)H_1(j2\omega)H_1(j3\omega) \quad (42)$$

$$G_4^H(j2\omega)=H_4(-j\omega,j\omega,j\omega,j\omega)=-\omega_L^2H_1(j2\omega)\big[\varepsilon_2H_{42}(j2\omega)+\varepsilon_4H_{44}(j2\omega)\big] \quad (43)$$

$$G_4^H(j4\omega)=H_4(j\omega,j\omega,j\omega,j\omega)=-\omega_L^2H_1(j4\omega)\big[\varepsilon_2H_{42}(j4\omega)+\varepsilon_4H_{44}(j4\omega)\big] \quad (44)$$

where

$$H_{42}(j2\omega)=H_{42}(j\omega,j\omega,j\omega,j\omega)=\omega_L^2\varepsilon_2^2\big\{\omega_L^2\big[H_1(j2\omega)H_1(j3\omega)+H_1(j\omega)H_1(j2\omega)\big]$$
$$+2H_1(j\omega)\big\}H_1^2(j\omega)\,|\,H_1(j\omega)\,|^2+\frac{1}{3}\varepsilon_2^2\,|\,H_1(j\omega)\,|^4\,\big[\omega_L^4\,|\,H_1(j2\omega)\,|^2+2\big] \quad (45)$$

$$H_{44}(j2\omega)=H_{44}(-j\omega,j\omega,j\omega,j\omega)=H_1^2(j\omega)\,|\,H_1(j\omega)\,|^2 \quad (46)$$

$$H_{42}(j4\omega)=H_{42}(j\omega,j\omega,j\omega,j\omega)=\omega_L^4\varepsilon_2^2H_1^4(j\omega)H_1(j2\omega)\big[4H_1(j3\omega)+H_1(j2\omega)\big] \quad (47)$$

$$H_{44}(j4\omega)=H_{44}(j\omega,j\omega,j\omega,j\omega)=H_1^4(j\omega) \quad (48)$$

4 Frequency Domain Energy Transfer of Bilinear Oscillators under Harmonic Loadings

4.1 General Analysis

It is well known that nonlinear systems subject to a harmonic input can generate higher order harmonic output components, and consequently transfer signal energy from the input frequency to higher order harmonics in the output. The introduction of the NOFRF concept can clearly explain and even predict how and when this phenomenon happens. Equations (25) and (29) indicate that if $N = 4$, then the 2nd, 3rd and 4th order harmonics could appear in the system output frequency response, and the output spectrum can analytically be described as

$$Y(j\omega_F) = G_1^H(j\omega_F)A_1(j\omega_F) + G_3^H(j\omega_F)A_3(j\omega_F) \quad (49)$$

$$Y(j2\omega_F) = G_2^H(j2\omega_F)A_2(j2\omega_F) + G_4^H(j2\omega_F)A_4(j2\omega_F) \quad (50)$$

$$Y(j3\omega_F) = G_3^H(j3\omega_F)A_3(j3\omega_F) \quad (51)$$

$$Y(j4\omega_F) = G_4^H(j4\omega_F)A_4(j4\omega_F) \quad (52)$$

Equations (50)~(52) clearly show how the higher order harmonics are generated. This is a combined effect of the system characteristics reflected by the NOFRF $G_n^H(j\omega)$ and the spectrum of the harmonic input raised to power n given by A_n for $n = 2,3,4$. In addition, by taking into account the specific expressions for $G_2^H(j2\omega)$, $G_3^H(j3\omega)$, $G_4^H(j2\omega)$ and $G_4^H(j4\omega)$ given by Equations (40) and (42)~(44), situation where a strong harmonic component can appear in the output of a bilinear oscillator can be easily predicted. Because $H_1(j\omega)$ of system (32) has only one resonance at the frequency ω_L, $H_1(jk\omega)$ will have one resonance at the frequency ω_L/k. Therefore the resonances of $H_1(j2\omega)$, $H_1(j3\omega)$ and $H_1(j4\omega)$ occur at $\omega_L/2$, $\omega_L/3$ and $\omega_L/4$ respectively. Equation (40) shows that $G_2^H(j2\omega)$ contains terms of $H_1(j\omega)$ and $H_1(j2\omega)$. Consequently, this may produce two resonance outputs at ω_L and $\omega_L/2$. Similarly, from Equation (41)~(48), $G_3^H(j3\omega)$ may produce three resonances at ω_L, $\omega_L/2$ and $\omega_L/3$; $G_4^H(j2\omega)$ has three possible resonances at ω_L, $\omega_L/2$ and $\omega_L/3$; and $G_4^H(j4\omega)$ has four possible resonances at ω_L, $\omega_L/2$, $\omega_L/3$ and $\omega_L/4$.

It is known from equations (50)~(52) that when the driving frequency ω_F coincides with one of these resonant frequencies of the NOFRFs, a significant amplitude in the output maybe produced corresponding to the higher order harmonic components. Consequently, considerable input signal energy may be transferred from the driving frequency to the higher order harmonic components in the output. For example, under the case when $\omega = \omega_F = \omega_L/2$, that is, the resonant frequency $\omega_L/2$ of $G_3^H(j3\omega)$ is reached. It is known from (51) that a considerable amplitude can be expected at the output frequency $3\omega_F = 3\omega_L/2$, because the system could transfer input energy from the driving frequency $\omega_L/2$ to frequency $3\omega_L/2$ in the output. These observations lead to a novel interpretation regarding when significant energy transfer phenomena may take place with a bilinear oscillator subjected to a harmonic input. The interpretation is based on the concept of resonant frequencies of NOFRFs, and concludes that significant energy transfer phenomena may occur with a bilinear oscillator when the driving frequency of the harmonic input happens to be one of the resonances of the NOFRFs.

This conclusion is likely to be significant in many aspects including both system design and fault diagnosis. Simulation studies will be conducted in the following section to demonstrate and justify this analysis.

4.2 Simulation Studies

The objective of the simulation studies is to demonstrate the effect of the resonances of the NOFRFs on the energy transfer phenomena of a bilinear oscillator when subjected to harmonic inputs. The analysis is important for system design. In addition, the effect of the stiffness ratio α, which defines the oscillator nonlinearity, will also be investigated to show how the NOFRFs change with the stiffness ratio. These results will form the basis of the use of a new system fault diagnosis method based on the NOFRFs.

Consider the bilinear oscillator equation (1) with parameters

$$m = 1\text{kg},\ \ k = 3.55\times10^{4}\ \text{N s/m},\ \ c = 23.5619\ \text{N/m}.$$

and the stiffness ratio changing between 1.0 and 0.8. The external force $f(t)$ considered was a sinusoidal type force with unit amplitude and frequency ω_F within the range $0 \le \omega_F \le 1.2\omega_0$. The simulation studies were conducted by integrating equation (1) using a fourth-order *Runge–Kutta* method to obtain the forced response of the system. The analysis in the previous sections indicates that when the system nonlinearity up to fourth order is taken into account, the spectrum of the forced system response can be described by equations (50)~(52).

From these relationships, it is known that the NOFRFs $G_3^H(j3\omega_F)$ and $G_4^H(j4\omega_F)$ can be determined using the algorithm in [19] with only one level of input excitation. Two levels input of excitations are required to determine the NOFRFs $G_1^H(j\omega_F)$, $G_3^H(j\omega_F)$, $G_2^H(j2\omega_F)$ and $G_4^H(j2\omega_F)$. Therefore, for each stiffness ratio α and at each frequency ω_F of the applied input, two forced responses were obtained with the magnitude of the sinusoidal input taken as $1N$ and $2N$ respectively, and, from the obtained responses, $G_1^H(j\omega_F)$, $G_3^H(j\omega_F)$, $G_2^H(j2\omega_F)$, $G_4^H(j2\omega_F)$, $G_3^H(j3\omega_F)$ and $G_4^H(j4\omega_F)$ were then determined using the algorithm in [19].

Figures 6~11 show the amplitudes of these NOFRFs at five different stiffness ratios of 0.8, 0.85, 0.9, 0.95 and 1.0 and over the range of frequencies of $0 \le \omega_F / \omega_0 \le 1.2$. From these figures, the resonances of the NOFRFs can be determined, and the results are given in Table 3~8. According to the analysis in Section 4.1, the resonances of $G_2^H(j2\omega_F)$, $G_4^H(j2\omega_F)$, $G_3^H(j3\omega_F)$ and $G_4^H(j4\omega_F)$ given in Table 5~8 imply that

(1) A significant second order harmonic could be observed when the driving frequency ω_F is about $\frac{1}{2}\omega_0$, the dominant resonance of $G_2^H(j2\omega_F)$ and $G_4^H(j2\omega_F)$.

(2) A significant third order harmonic may appear when the driving frequency ω_F is about $\frac{1}{3}\omega_0$, the dominant resonance of $G_3^H(j3\omega_F)$.

(3) A significant fourth order harmonic may appear when the driving frequency ω_F is about $\frac{1}{4}\omega_0$, the dominant resonance of $G_4^H(j4\omega_F)$.

In order to justify these conclusions from the general NOFRF based analysis, the output spectra of the bilinear oscillator subjected to harmonic inputs at the frequencies of $\omega_F = 1/6\omega_0$, $\omega_F = 1/3\omega_0$ and $\omega_F = 1/2\omega_0$, respectively, were determined, the results are shown in Figure 12. It can be seen from Figure 12(a) that at $\omega_F = 1/6\omega_0$, all higher order harmonics, including the second harmonic, are very weak, especially the third order harmonic which can hardly be seen. This is simply because in this case $\omega_F = 1/6\omega_0$ is not a resonant frequency of any of the NOFRF involved in the expression for the system output spectrum. From Figure 12(b) where $\omega_F = 1/3\omega_0$, the dominant resonance of $G_3^H(j3\omega_F)$, it is known that the third order harmonic becomes manifest. This can be explained by equation (51) which indicates that a significant third order harmonic could be observed in the system output response. From Figure 12(c) where $\omega_F = 1/2\omega_0$, the dominant resonances of $G_2^H(j2\omega_F)$ and $G_4^H(j2\omega_F)$, it can be observed that although the third order harmonic is visible, its amplitude is smaller than that in Figure 12(b). This is because, as shown in Figure 10, although $\omega_F = 1/2\omega_0$ is a resonant frequency of $G_3^H(j3\omega_F)$, it is not the dominant resonant frequency. However, Figure 12(c) shows that, the second order harmonic is significant. This result is completely consistent with the analysis one can achieve from equation (50) which shows the effects of the 2$^{\text{nd}}$ harmonic can be extremely important when ω_F happens to be the dominant resonances of $G_2^H(j2\omega_F)$ and $G_4^H(j2\omega_F)$.

In mechanical engineering studies [28], the appearance of superharmonic components in the output spectrum is considered to be a significant nonlinear effect. From the perspective of the energy transfer, it is the linear FRF which transfers the input energy to the fundamental harmonic component in the output spectrum, and it is the NOFRFs which transfer the input energy to the superharmonic components. Therefore, to a certain extent, one can think that if the superharmonic components contain more energy in the output spectrum, then the nonlinear effect of the bilinear oscillator is stronger. Figure 13 shows the percentage of the whole energy that the superharmonic components contain at different frequencies for different stiffness ratios. It can be seen that around the frequency of $1/2\omega_0$, the superharmonic components have the biggest percentage of the total energy. This implies that, when a bilinear oscillator works around half the natural frequency, more energy will be transferred to the superharmonic frequency locations, and the bilinear oscillator will thus render the strongest nonlinear phenomenon. This result again confirms the analysis result that can be obtained from equation (50) about the effects of the resonances of $G_2^H(j2\omega_F)$ and $G_4^H(j2\omega_F)$ on the system frequency domain energy transfer phenomenon. In addition, two weak peaks appear in Figure 13 around the frequencies of $\omega_F = 1/3\omega_0$ and $\omega_F = 1/4\omega_0$, which is especially obvious in the case of stiffness ratio $\alpha = 0.8$. This is due to the effect of the dominant resonance of $G_3^H(j3\omega_F)$ and $G_4^H(j4\omega_F)$ as indicated by equations (51) and (52).

In engineering practice and laboratory research activities [13][29][30], people have observed that, when the excitation frequency passes through the half eigenfrequency of a cracked object, the vibration becomes more severe. This phenomenon is known as secondary resonance. As a cracked element can often be modelled as a spring with a bilinear stiffness, it is known now that the secondary resonance is actually produced by the dominant resonances of two NOFRFs $G_2^H(j2\omega_F)$ and $G_4^H(j2\omega_F)$. Therefore the NOFRF based analysis in the present study provides an alternative and more general interpretation for the well-known phenomenon of the secondary resonance in cracked objects. Furthermore, it can be expected that there would exist 3rd, and 4th, etc. resonances. However, compared with $G_2^H(j2\omega_F)$ and $G_4^H(j2\omega_F)$, the amplitudes of the dominant resonances of $G_3^H(j3\omega_F)$ and $G_4^H(j4\omega_F)$ are relatively small, moreover, the amplitudes of $A_i(j\omega)$, i=1,…,4 decrease with the order number i, therefore the effects from the 3rd and 4th, etc. resonances are often not so manifest.

All the above analysis results verify the general analysis given in Section 4.1, and reveal the significant effect of the resonances of NOFRFs on the energy transfer phenomena of bilinear oscillators. These NOFRFs' resonance based analysis for the energy transfer phenomenon of bilinear oscillators can be directly used in system design. Given the driving frequencies of possible harmonic loadings with a bilinear oscillator, if the objective for the oscillator design is to reduce the energy of higher order harmonic components, then the analysis implies that the natural frequency of the linear part of the oscillator $\omega_L = \sqrt{c_1 k/m} = \sqrt{c_1}\omega_0 \approx \omega_0$ has to be designed such that no frequencies of possible harmonic loadings may happen to be resonances of associated NOFRFs, which, for the specific cases above, are ω_0, $1/2\omega_0$, $1/3\omega_0$ and $1/4\omega_0$.

In addition to the resonances of the NOFRFs, from Figures 6~11, the relationship between the stiffness ratio and the NOFRFs can also be observed; the dependence of the NOFRFs on the stiffness ratio is more clearly manifest by the magnitudes of NOFRFs at the resonant frequencies. Because many cracked rotors and beams can be modelled as a bilinear oscillator and the stiffness ratio in the oscillator model represents the size of cracks, the NOFRFs of the rotors and beams at resonances are a significant indicator. Therefore, there is considerable potential to use the NOFRFs evaluated at their resonances to conduct fault diagnosis and estimation for these mechanical systems and structures.

5 Conclusion

This paper presents an analysis of the energy transfer phenomenon of bilinear oscillators in the frequency domain using the NOFRF concept recently developed by the authors. It is verified that a bilinear oscillator can be approximated by a fourth-order polynomial-type nonlinear model, which can easily be analyzed using the Volterra series theory of nonlinear systems. The NOFRF concept is then used to analyze the forced response of a bilinear oscillator subjected to a sinusoidal excitation. The results of the analysis reveal, for the first time, that when the frequency ω_F of the input force is close to the resonances of the associated NOFRFs, such as $1/2\omega_0$, $1/3\omega_0$ and $1/4\omega_0$, etc, considerable input energy will be transferred to the superharmonic locations of $2\omega_F$, $3\omega_F$ and $4\omega_F$, etc. This is an important conclusion regarding when the phenomenon of new frequency generation may occur with bilinear oscillators, and is of practical significance for the system design. In addition, it is demonstrated that the magnitudes of the NOFRFs at the resonances are a significant indicator of the value of the stiffness ratio in the bilinear oscillator model. Because the stiffness ratio is directly related to the crack size of cracked mechanical systems and structures which can be modelled by a bilinear oscillator, the NOFRF based analysis has a great potential in mechanical system fault diagnosis.

Acknowledgements

The authors gratefully acknowledge the support of the Engineering and Physical Science Research Council, UK, for this work.

References

1. J. M. T Thompson, A. R Bokaian, R. Ghaffari, Subharmonic resonances and chaotic motions of a bilinear oscillator, *IMA Journal of Applied Mathematics* 31 (1983) 207-234.
2. M. Gerber, L. Engelbrecht, The bilinear oscillator: The response of an articulated mooring tower driven by irregular seas, *Ocean Engineering* 20 (1993) 113-133.
3. Y. M. Huang, C. M. Krousgrill, A. K. Bajaj, Dynamic behaviour of offshore structures with bilinear stiffness, *Journal of Fluids and Structures* 3 (1989) 405-422.
4. H. S Choi, J. Y. K Lou, Nonlinear behaviour and chaotic motions of an SDOF system with piecewise-non-linear stiffness, *International Journal of Non-Linear Mechanics* 26 (1991) 461-473.
5. J. F. Wilson, E. G. Callis, The dynamics of loosely jointed structures, *International Journal of Non-Linear Mechanics* 39 (2004) 503-514.
6. E. A. Butcher, Clearance effects on bilinear normal mode frequencies, *Journal of Sound and Vibration* 224 (1999) 305-328.
7. B. Zastrau, Vibrations of cracked structures, *Archives of Mechanics* 37 (1985) 731-743.
8. M. I. Friswell, J. E. T. Penny, A simple nonlinear model of a cracked beam. *Proceedings* 10*th International Modal Analysis Conference*, *San Diego*, CA 1, (1992) 516-521.
9. J. N. Sundermeyer, R. L. Weaver, On crack identification and characterization in a beam by non-linear vibration analysis, *Journal of Sound and Vibration* 183 (1995) 857-871.
10. A. Rivola, P. R. White, Bispectral analysis of the bilinear oscillator with application to the detection of fatigue cracks, *Journal of Sound and Vibration* 216 (1998) 889-910.
11. M. Chati, R. Rand and S. Mukherjee, Modal analysis of a cracked beam, *Journal of Sound and Vibration* 207 (1997) 249-270.
12. R. Gasch, Dynamic behaviour of a simple rotor with a cross-sectional crack, *IMechE Conference on Vibrations in Rotating Machinery* (1976) 123–128.
13. R. Gasch, A survey of the dynamic behaviour of a simple rotating shaft with a transverse crack, *Journal of Sound and Vibration* 160 (1993) 313–332.
14. S. Natsiavas, On the dynamics of oscillators with bilinear damping and stiffness, *International Journal of Non-Linear Mechanics* 25 (1990) 535-554
15. Y. C. Chu, M. H. H. Shen, Analysis of forced bilinear oscillators and the application to cracked beam dynamics, *AIAA Journal* 30 (1992) 2512-2519.

16. P. V. Bayly, On the spectral signature of weakly bilinear oscillators, *Journal of Vibration and Acoustics-Transactions of the ASME* 118 (1996) 352-361
17. Z. Q. Lang, S. A. Billings, Output frequency characteristics of nonlinear system, *International Journal of Control* 64 (1996) 1049-1067.
18. S. A. Billings, Z. Q. Lang, Non-linear systems in the frequency domain: energy transfer filters, *International Journal of Control* 75 (2002) 1066-1081.
19. Z. Q. Lang, S. A. Billings, Energy transfer properties of nonlinear systems in the frequency domain, *International Journal of Control* 78 (2005) 354-362.
20. G. M. Lee, Estimation of non-linear system parameters using higher-order frequency response functions, *Mechanical Systems and Signal Processing* 11 (1997) 219-229.
21. H. Jeffreys, B. S. Jeffreys *Methods of Mathematical Physics, 3rd ed.* 1988 Cambridge, England: Cambridge University Press.
22. H. Zhang, S. A. Billings, Analysing non-linear systems in the frequency domain, I: the transfer function, *Mechanical Systems and Signal Processing* 7 (1993) 531–550.
23. H. Zhang, S. A. Billings, Analysing nonlinear systems in the frequency domain, II: the phase response, *Mechanical Systems and Signal Processing* 8 (1994) 45–62.
24. J. A. Vazquez Feijoo, K. Worden, R. Stanway, Associated Linear Equations for Volterra operators, *Mechanical Systems and Signal Processing* 19 (2005) 57-69.
25. J. A. Vazquez Feijoo, K. Worden. R. Stanway, System identification using associated linear equations, *Mechanical Systems and Signal Processing* 18 (2004) 431-455.
26. J.A. Vazquez Feijoo, K. Worden, R. Stanway, Analysis of time-invariant systems in the time and frequency domain by associated linear equations (ALEs), *Mechanical Systems and Signal Processing* (2005) In press
27. S. A. Billings, J. C. Peyton-Jones, Mapping nonlinear integro-differential equation into the frequency domain, *International Journal of Control* 54 (1990) 863-879.
28. A.P. Bovsunovskya, C. Surace, Considerations regarding superharmonic vibrations of a cracked beam and the variation in damping caused by the presence of the crack, *Journal of Sound and Vibration* (2005) In press
29. N. Pugno, R. Ruotolo, C. Surace, Analysis of the harmonic vibrations of a beam with a breathing crack, *Proceedings of the 15th IMAC*, Tokyo, Japan, (1997) 409-413.
30. A.K. Darpe, K. Gupta, A. Chawla, Transient response and breathing behaviour of a cracked Jeffcott rotor, *Journal of Sound and Vibration* 272 (2004) 207-243

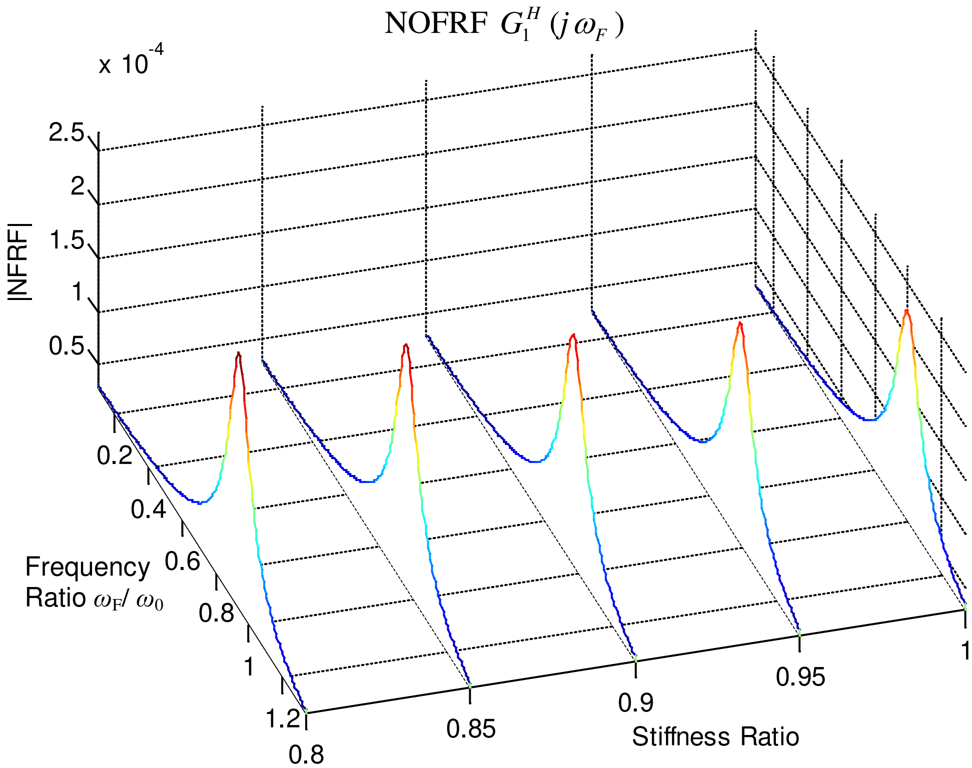

Figure 6 NOFRFs $G_1^H(j\omega_F)$ at different stiffness ratios

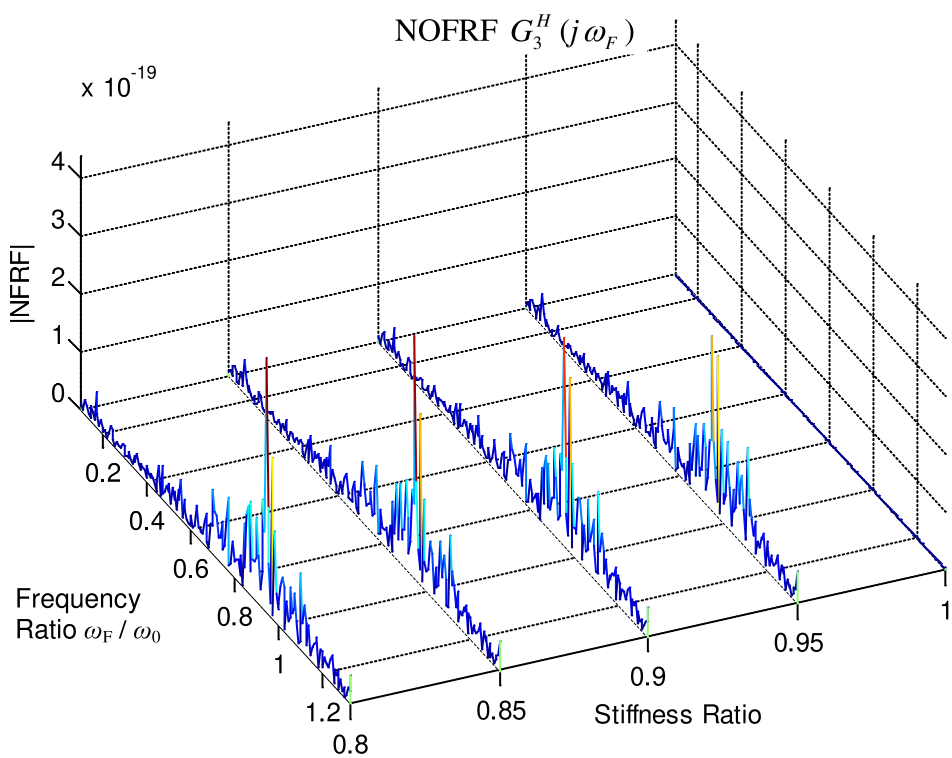

Figure 7 NOFRFs $G_3^H(j\omega_F)$ at different stiffness ratios

NOFRF $G_2^H(j2\omega_F)$

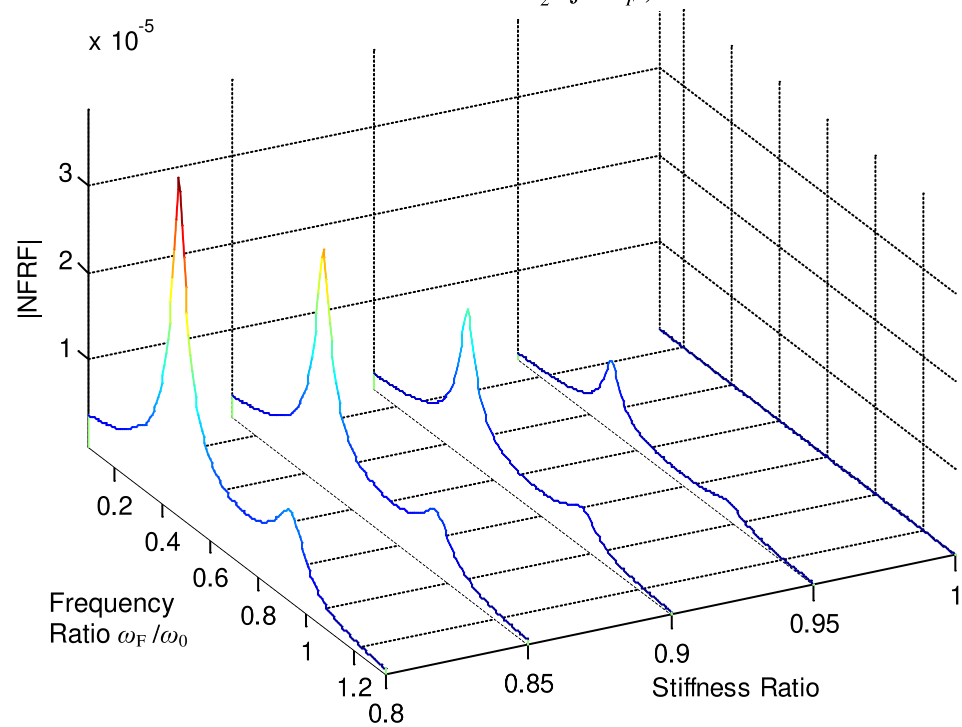

Figure 8 NOFRFs $G_2^H(j2\omega_F)$ at different stiffness ratios

NOFRF $G_4^H(j2\omega_F)$

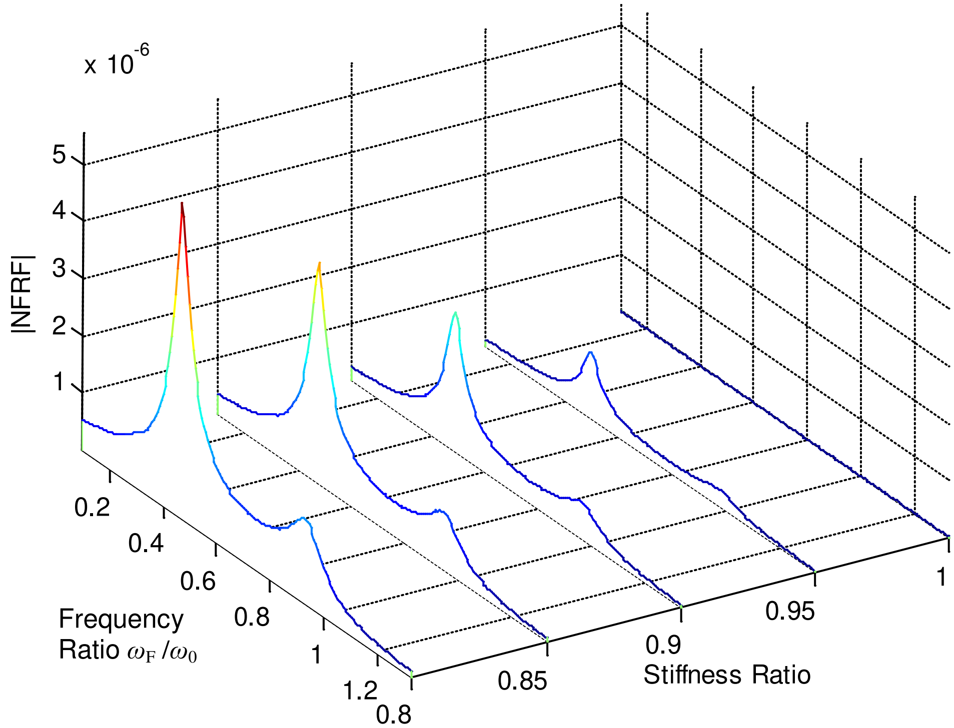

Figure 9 NOFRFs $G_4^H(j2\omega_F)$ at different stiffness ratios

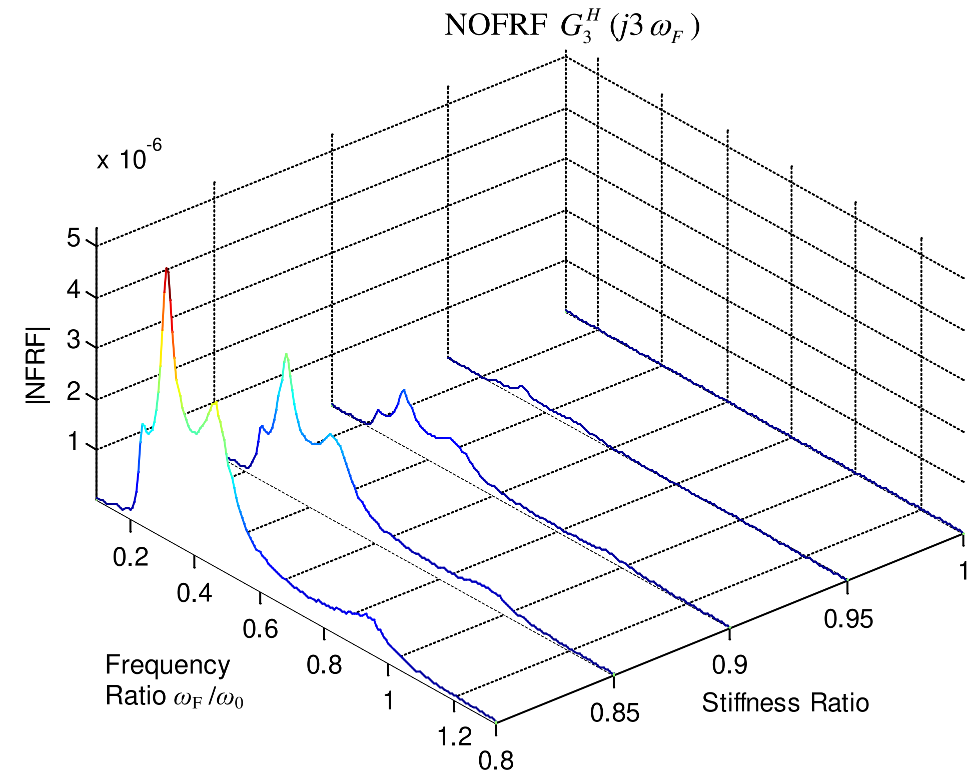

Figure 10 NOFRFs $G_3^H(j3\omega_F)$ at different stiffness ratios

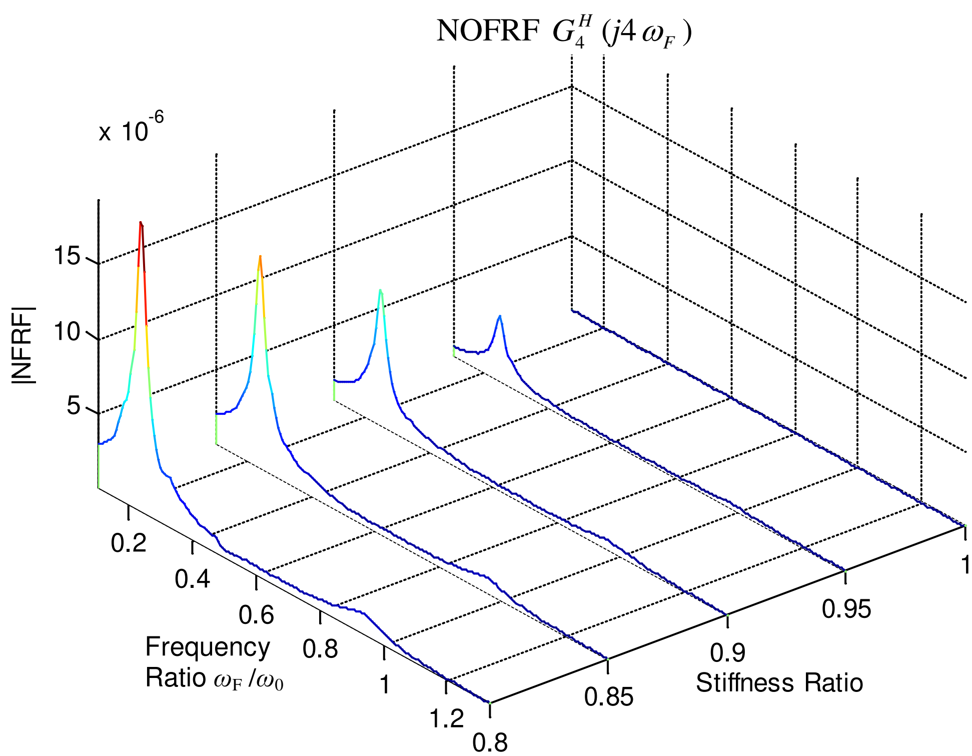

Figure 11 NOFRFs $G_4^H(j4\omega_F)$ at different stiffness ratios

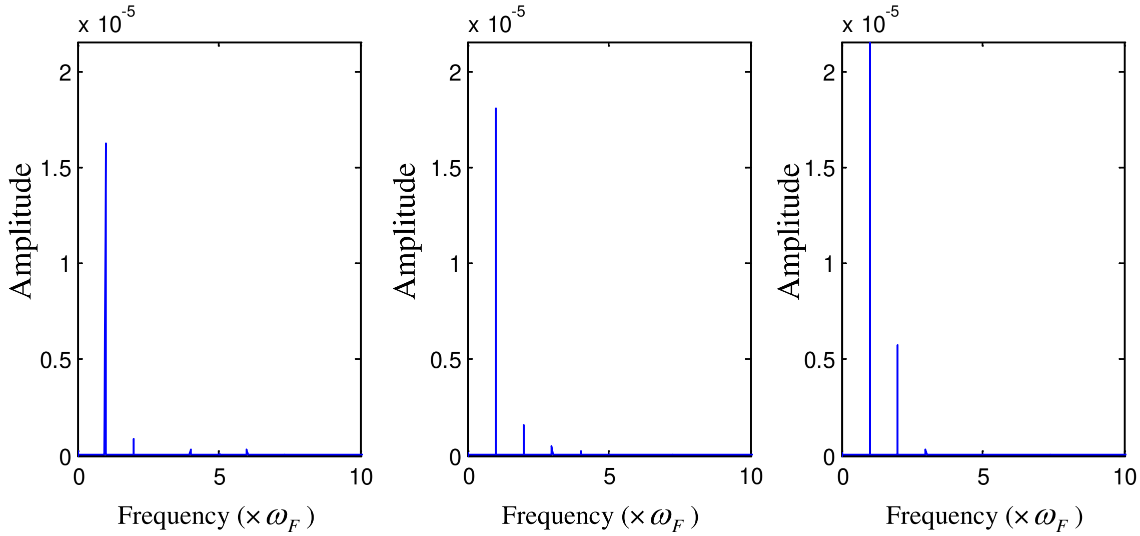

(a) $\omega_F = 1/6\omega_0$ (b) $\omega_F = 1/3\omega_0$ (c) $\omega_F = 1/2\omega_0$

Figure 12 The spectra of the output at different frequencies ($\alpha = 0.8$)

Table 3 Resonance of $G_1^H(j\omega_F)$

Stiffness Ratio	**First Resonance**	
	Frequency ($\times\omega_0$)	Amplitude
0.80	0.94667	2.6748e-4
0.85	0.95333	2.5509e-4
0.90	0.96667	2.4450e-4
0.95	0.98667	2.3423e-4
1.00	1.00000	2.2545e-4

Table 4 Resonance of $G_3^H(j\omega_F)$

Stiffness Ratio	**First Resonance**	
	Frequency ($\times\omega_0$)	Amplitude
0.80	0.9400	4.3827e-19
0.85	0.9533	4.1928e-19
0.90	0.9667	1.5892e-19
0.95	0.9867	1.7522e-19
1.00	1.0000	0.0000e-19

Table 5 Resonances of $G_2^H(j2\omega_F)$

Stiffness Ratio	First Resonance		Second Resonance	
	Frequency ($\times\omega_0$)	Amplitude	Frequency ($\times\omega_0$)	Amplitude
0.80	0.9467	1.0290e-5	0.4733	3.8824e-5
0.85	0.9533	7.1957e-6	0.4800	2.7317e-5
0.90	0.9667	4.4698e-6	0.4867	1.7116e-5
0.95	0.9867	2.0882e-6	0.4933	8.0414e-6
1.00	NaN	NaN	NaN	NaN

Table 6 Resonances of $G_4^H(j2\omega_F)$

Stiffness Ratio	First Resonance		Second Resonance	
	Frequency ($\times\omega_0$)	Amplitude	Frequency ($\times\omega_0$)	Amplitude
0.80	0.9467	1.4701e-6	0.4733	5.5466e-6
0.85	0.9533	1.0280e-6	0.4800	3.9027e-6
0.90	0.9667	6.3856e-7	0.4867	2.4453e-6
0.95	0.9867	2.9832e-7	0.4933	1.1488e-6
1.00	NaN	NaN	NaN	NaN

Table 7 Resonances of $G_3^H(j3\omega_F)$

Stiffness Ratio	First Resonance		Second Resonance		Third Resonance	
	Frequency ($\times\omega_0$)	Amplitude	Frequency ($\times\omega_0$)	Amplitude	Frequency ($\times\omega_0$)	Amplitude
0.80	0.9467	7.0983e-7	0.4733	3.2564e-6	0.3133	5.3510e-6
0.85	0.9533	3.5522e-7	0.4800	1.6534e-6	0.3200	2.7400e-6
0.90	0.9667	1.6106e-7	0.4667	6.7182e-7	0.3267	1.1055e-6
0.95	0.9867	3.8108e-8	0.4933	1.5098e-7	0.3333	2.4882e-7
1.00	NaN	NaN	NaN	NaN	NaN	NaN

Table 8 Resonances of $G_4^H(j4\omega_F)$

Stiffness Ratio	First Resonance		Second Resonance	
	Frequency ($\times\omega_0$)	Amplitude	Frequency ($\times\omega_0$)	Amplitude
0.80	0.9467	1.4182e-6	0.2333	1.9339e-5
0.85	0.9533	1.0412e-6	0.2400	1.4268e-5
0.90	0.9667	6.6331e-7	0.2400	8.9509e-6
0.95	0.9867	3.1042e-7	0.2467	4.2988e-6
1.00	NaN	NaN	NaN	NaN

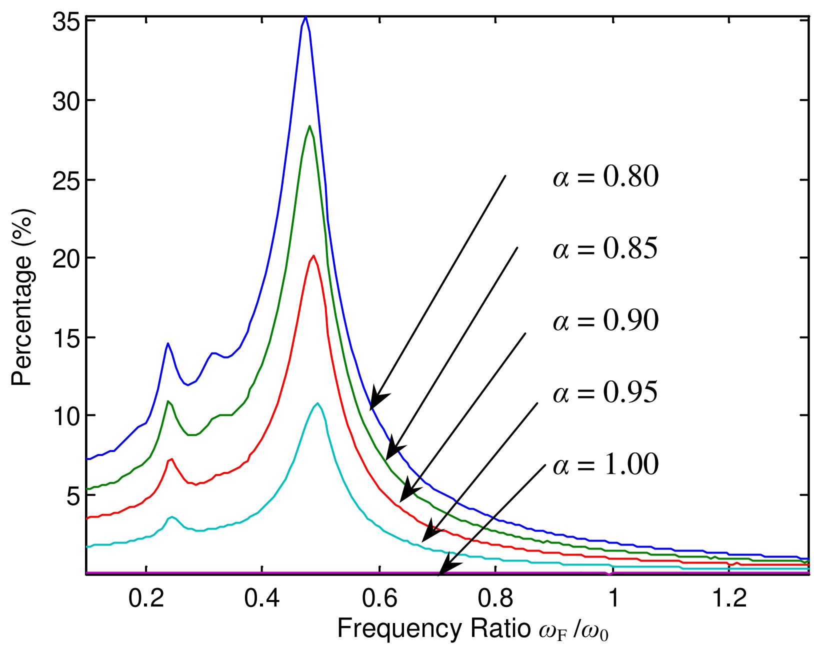

Figure 13 The percentage of the whole energy that the superharmonic components contain at different frequencies for different stiffness ratios